JOURNAL OF PHYSICAL ORGANIC CHEMISTRY, VOL. 5, 179–190 (1992)

MULTI-STEP PROCESSES IN GAS-PHASE REACTIONS OF HALOMETHYL ANIONS XCH_2^- (X=Cl,Br) WITH CH_3X AND NH_3

F. MATTHIAS BICKELHAUPT, LEO J. DE KONING AND NICO M. M. NIBBERING*
Intituut voor Massaspectrometrie, Universiteit van Amsterdam, Nieuwe Achtergracht 129, 1018 WS Amsterdam, The Netherlands

EVERT JAN BAERENDS
Scheikundig Laboratorium, Vrije Universiteit, De Boelelaan 1083, 1081 HV Amsterdam, The Netherlands

A mechanistic investigation of the gas-phase reactivity of the halomethyl anions XCH_2^-(X=Cl, Br) towards a mixture of the corresponding halomethane and ammonia was performed using Fourier transform ion cyclotron resonance mass spectrometry. The interpretation of the experimental data is supported by high-level density functional theoretical (DFT) calculations for the chlorine-containing systems (X=Cl). When the specific isotopomer $^AXCH_2^-$ ($^AX=^{35}Cl$, ^{79}Br) is allowed to react in an atmosphere of CH_3X and NH_3, the exclusive formation of the isotope cluster of the halide anions $^AX^-$ and $^BX^-$($^BX=^{37}Cl$, ^{81}Br) is observed. However, the intensity ratio $I(^AX^-)/I(^BX^-)$ exceeds significantly the value expected from the natural relative isotope abundances and depends linearly on the pressure ratio $p(NH_3)/p(CH_3X)$. The experimental results are interpreted in terms of three competing reaction mechanisms: (i) The by far dominating process is the more than 70 kcal mol^{-1} exothermic one-step S_N2 substitution of $^AXCH_2^-$ on CH_3X, generating haloethane $^AXCH_2CH_3$ and X^- isotopomers, the latter in the proportion of their natural abundances (direct S_N2). The experimentally observed excess of $^AX^-$ stems from two minor reaction pathways: (ii) in a secondary reaction, the halide X^- in the primary product anion–molecule complex $[^AXCH_2CH_3\cdots X^-]^*$ of the S_N2 substitution induces a 1,2-elimination, leading to the formation of the $^AX^-$ isotopomer (two-step $S_N2/E2$). (iii) Finally, $^AXCH_2^-$ can react with ammonia by consecutive endothermic proton transfer (PT) from NH_3 to $^AXCH_2^-$ and a very exothermic S_N2 substitution of the resulting amide on $^AXCH_3$ leading to CH_3NH_2 and an excess of $^AX^-$ which depends linearly on $p(NH_3)/p(CH_3X)$ (PT/S_N2). Theoretical calculations show that in the case of $[ClCH_2^-\cdots NH_3]^*$, the PT/S_N2 reaction has no stable intermediate. Therefore, it is concluded that this reaction is *not* a two-step but a one-step process.

INTRODUCTION

In the past decade, a large number of gas-phase ion-molecule reactions have been studied by Fourier transform ion cyclotron resonance (FT-ICR) mass spectrometry, and it has been well established that the observed gas-phase ion–molecule reactions proceed via loose ion–molecule complexes which are bound by ion–dipole and ion–induced dipole interactions and hydrogen bonds.[1,2] A fascinating phenomenon is the possibility of secondary reactions taking place in relatively long lived product ion–molecule complexes of primary reactions, i.e. product ions can be formed via multiple consecutive reaction steps.[3,4]

In this context, an interesting observation has been reported by our group in a study on the gas-phase reactivity of a number of carbanions bearing an α-heteroatom.[5] In that study, amongst others, the reactivity of the halomethyl anions $ClCH_2^-$ and $BrCH_2^-$ was investigated in an atmosphere of the corresponding halomethane and ammonia. When $^{35}ClCH_2^-$ was isolated and subsequently allowed to react, no $^{37}ClCH_2^-$ ions were formed. However, $^{35}Cl^-$ was produced more abundantly than expected from S_N2 substitution on chloromethane, i.e. the intensity ratio $I(^{35}Cl^-)/I(^{37}Cl^-)$ significantly exceeded the natural relative isotope abundance[6] of 3.13 [equation (1)].

$$^{35}ClCH_2^- \xrightarrow{CH_3Cl-NH_3} \begin{cases} \longrightarrow {}^{35}Cl^- : {}^{37}Cl^- > 3:1 & \text{(1a)} \\ \not\longrightarrow {}^{37}ClCH_2^- & \text{(1b)} \end{cases}$$

This was explained by proposing[5] a mechanism in which the chloromethyl anion, $^{35}ClCH_2^-$, reacts with ammonia via a two-step mechanism: (i) in the first step

* Author for correspondence.

0894–3230/92/040179–12$06.00

Received 28 August 1991
Revised 9 December 1991

the intermediate complex $[^{35}ClCH_3\cdots NH_2^-]^*$ is formed by endothermic proton transfer (PT) from ammonia to $^{35}ClCH_2^-$; (ii) in the second step, the amide NH_2^- effects an S_N2 substitution under expulsion of the $^{35}Cl^-$ [equation (2); R=H]. Support for this mechanism comes from the observation that the addition of a more acidic amine R_2NH leads to an increase in the excess of $^{35}Cl^-$. Similar results were obtained for $^{79}BrCH_2^-$ in an atmosphere of bromomethane and an amine.

$$^{35}ClCH_2^- + R_2NH \leftrightharpoons [^{35}ClCH_2^-\cdots R_2NH]^* \leftrightharpoons [^{35}ClCH_3\cdots R_2N^-]^* \rightarrow {}^{35}Cl^- + CH_3NR_2 \quad (2)$$

The purpose of this work was a quantitative elucidation of the different mechanisms which contribute to the above-mentioned formation of the halide anion isotope cluster in a combined FT-ICR mass spectrometric and density-functional theoretical (DFT) approach. To this end, several *a priori* conceivable mechanisms are discussed and a relationship is presented which expresses the isotope intensity ratio $I(^AX^-)/I(^BX^-)$ as a function of the pressure ratio $p(NH_3)/p(CH_3X)$. This relationship serves a the guide for the mass spectrometric experiments and for the interpretation of their results.

In addition to the eludication and quantification of the mechanisms active in the chloride or bromide anion formation, the nature of these mechanisms was investigated by theoretical calculations, using a high-level density-functional (DF) method as implemented in the Amsterdam DF program system.[7-12] One question which will be addressed concerns the character of the PT/S_N2 reaction: does a stable intermediate $[^{35}ClCH_3\cdots R_2N^-]^*$ exist as postulated in equation (2)? This might not be the case[13] for a proton transfer which is endothermic by 7·6 kcal mol^{-1} (1 kcal = 4·184 kJ).[14] Further, an explanation is presented for the observation that a thermoneutral PT in the reactant complex $[^{35}ClCH_2^-\cdots CH_3Cl]^*$ cannot compete with the S_N2 process. For economic reasons the theoretical investigations do not include the bromine-containing systems.

EXPERIMENTAL

The experiments were performed with a laboratory-constructed Fourier transform ion cyclotron resonance (FT-ICR) mass spectrometer equipped with a 1·2 T electromagnet and a cubic inch cell.[15] The segmented Fourier transform (SEFT) procedure[16] was employed in all cases to obtain absolute peak intensities with an accuracy of better than 5%. General operating and experimental procedures have been described previously.[15]

The temperature in the cell was *ca* 333 K as measured by a thermocouple on the trapping plate opposite the filament. The total pressure in the different experiments was kept between 10^{-6} and 10^{-4} Pa with a background pressure lower than 5×10^{-7} Pa. The pressures were measured with an ionization gauge manometer placed in a side-arm of the main pumping line. The ionization gauge manometer was calibrated for methane by fitting our rate constant for the reaction $CH_4^{+\cdot} + CH_4 \rightarrow CH_5^+ + CH_3^\cdot$ to the average literature value of $(1\cdot11 \pm 0\cdot04)\times10^{-9}$ cm^{3}molecule^{-1} s^{-1}.[17] Absolute pressures were obtained by correction for the relative sensitivities R_x of the ionization gauge manometer for gases x, using the relationship $R_x = 0\cdot36\alpha + 0\cdot30$ of Bartmess and Georgiadis[18] and polarizabilities α from Miller.[19]

NH_2^- was generated via dissociative resonant capture of electrons with a kinetic energy of 5 eV by ammonia. The halomethyl anions were formed through proton abstraction from the corresponding halomethane by NH_2^-. All the chemicals used were commercially available.

THEORETICAL

General

The MOs were expanded in a large set of Slater-type orbitals (STOs). The basis is of double-ζ quality (two STOs per nl shell). A polarization function was added on each atom: 2p on H, 3d on C, N, and Cl. Geometries were optimized with the simple Xα exchange-correlation potential[7] using gradient techniques.[20] C_s point group symmetry was assumed for the ion–molecule complexes. The energy data reported for stable structures (energy minima) were obtained in the optimum geometry with more sophisticated density-functionals (DF) for exchange and correlation. Exchange is described with Slater's $\rho^{1/3}$ potential (Xα with $\alpha = 2/3$), with a non-local correction due to Becke and co-workers.[21-23] According to the suggestion by Stoll *et al.*,[24] only correlation between electrons of different spin is introduced, for which electron gas data (in the Vosko–Wilk–Nusair[25] parametrization) are used.

Accuracy of DF interaction energies

Table 1 compares our DFT results for the cluster energies (ΔE_{clust}) and enthalpies (ΔH_{clust}) of a number of small anion–molecule complexes with the results obtained by other theoretical and experimental methods. The DFT cluster energies, ΔE_{clust}, are in good agreement with the results obtained by conventional *ab initio* calculations. For the $H_2O\cdots OH^-$ and $CH_4\cdots CH_3^-$ systems, incorporation of correlation into the conventional *ab initio* calculation leads to a strengthening of the anion–molecule interaction and to a better agreement with the DFT values. The DFT cluster enthalpies, ΔH_{clust}, also compare well with those obtained experimentally. Deviations are of the order of

Table 1. Comparison of the cluster energies (ΔE_{clust}) and enthalpies (ΔH_{clust}) (kcal mol^{-1}) of a number of small anion–molecule complexes as obtained by several theoretical and experimental methods

System	ΔE_{clust}		ΔH_{clust}(298 K)	
	DFT[a]	Other calculation	DFT[a,b]	Experiment
$ClH\cdots Cl^-$	−25·0[c]	−22·3[e]	−22·5	−23·9 ± 2[j]
$FH\cdots F^-$	−48·3[c,d]	−43·4[e]	−45·8	−38·7 ± 2[k]
$H_2O\cdots OH^-$	−35·0	−23·1,[f] −28·0[g]	−28·5	−23·9 ± 2,[l] −35·6 ± 6·9[m]
$NH_3\cdots NH_2^-$	−17·6	—	−11·1	−12[n]
$CH_4\cdots CH_3^-$	− 6·7	−1.40,[h] −2·35[i]	− 0·2	—

[a] This work; energy calculated with sophisticated density-functionals[21–25] in Xα geometry,[7] double-ζ STO basis with one polarization function on each atom (see text).
[b] $\Delta H_{clust}(T) \approx \Delta E_{clust} + \Delta ZPE + (5/2)RT$; the difference in zero-point vibrational energies between the cluster and the separated fragments, ΔZPE, is estimated from the literature:[32] for $ClH\cdots Cl^-$ and $FH\cdots F^-$ $\Delta ZPE \approx 1$ kcal mol^{-1}, for the other systems $\Delta ZPE \approx 5$ kcal mol^{-1}.
[c] Xα geometry optimization yields a $D_{\infty h}$ symmetric 'proton-bound' halide dimer structure.
[d] triple-ζ STO basis with two polarization functions on each atom: 3d and 4f on F and 2p and 3d on H.
[e] Minato and Yamabe,[39] HF with double-ζ plus polarization basis.
[f] Roos *et al.*,[33] HF with [541/31] basis.
[g] Roos *et al.*,[33] CI with [541/31] basis.
[h] Latajka and Scheiner,[34] HF with 6–31G** + p(C) basis [ζ_p(H) = 0·15].
[i] Latajka and Scheiner,[34] MP3 with 6–31G** + p(C) basis [ζ_p(H) = 0·15].
[j] Caldwell and Kebarle.[35]
[k] Larson and McMahon.[36]
[l] Payzant *et al.*[37]
[m] DePaz *et al.*[38]
[n] Lias *et al.*[14]

5 kcal mol^{-1}. The largest deviation is found for $FH\cdots F^-$, where the DFT value (−45·8 kcal mol^{-1}) is 7·1 kcal mol^{-1} more bonding than the experimental value[36] of −38·7 ± 2 kcal mol^{-1}. The cluster energy and enthalpy of the fluorine containing anion–molecule complex appear to depend very critically on the quality of the basis set. Therefore, the DFT calculation was performed with an extra large triple-ζ basis augmented with two polarization functions on each atom (3d and 4f on F, 2p and 3d on H). The difference of 7·1 kcal mol^{-1} between the DFT and experimental ΔH_{clust} might be further reduced if a quadruple-ζ basis is employed.

Summarizing, we conclude that with the DF approach interaction energies in anion–molecule complexes are described to an accuracy in the order of 5 kcal mol^{-1}, in agreement with previous experience on systems involving main group elements and/or metals.[20,26–31]

Determination of reaction paths

Reaction paths are determined by elongating the bond to be broken in steps of 10 pm (see Theoretical results). After each step the geometry is allowed to relax; however, the length of the elongated bond is kept fixed. The reaction paths and activation energies are calculated using the Xα exchange-correlation potential.

In a study on the cyanide–isocyanide isomerization of HCN and CH_3CN and the *E–Z* isomerization of N_2H_2, Fan and Ziegler[29] showed that with this level of density functional theory (DFT) activation energies are obtained which overestimate the barrier by about 5 kcal mol^{-1}. Conventional *ab initio* methods which take electron correlation into account to some extent (e.g. Hartree–Fock + many-body perturbation theory (HF + MBPT)) afford barriers that are 5–10 kcal mol^{-1} higher than the DFT values.[29] We have obtained similar results for the activation energy for proton transfer in $CH_4\cdots CH_3^-$, a system that closely resembles the anion–molecule complexes of present interest. The Xα exchange-correlation potential arrives at a barrier of 3·97 kcval mol^{-1}, while with the more sophisticated density-functionals (see above) the calculated barrier amounts to 9·59 kcal mol^{-1}. The latter is only about 3 kcal mol^{-1} lower than the best MP3 value of 12·86 kcal mol^{-1} obtained by Latajka and Scheiner[34] with a 6–31G** + p(C) basis set (at the HF level Latajka and Scheiner obtained a barrier of 21·98 kcal mol^{-1}).

SELECTION OF POSSIBLE REACTION MECHANISMS

In this section, several *a priori* conceivable mechanisms which can lead to the observed formation of the X^- isotope cluster in the reaction system $^AXCH_2^- + CH_3X + NH_3$ are presented. It will be discussed which of them is in principle suitable to be taken into account when an expression is derived which

relates the intensity ratio $I(^{A}X^{-})/I(^{B}X^{-})$ to the pressure ratio $p(CH_3X)/p(NH_3)$, and which serves as an instrument for the mechanistic investigation. From the fact that no $^{B}XCH_2^-$ ions are formed when $^{A}XCH_2^-$ is isolated and allowed to react in an atmosphere of CH_3X and NH_3, it is concluded that no measurable thermoneutral proton transfer (PT) occurs in the reactant complex $[^{A}XCH_2^- \cdots CH_3^{B}X]^*$. This point is explained in more detail under Discussion.

Conceptually the most simple process which results in the formation of the excess of $^{A}X^-$ is the bimolecularly induced dissociation of the selected halomethyl anion into methylene and the specific isotopomer of the halide anions [equation (3)]. However, on the basis of energetic considerations, this second step of an α-E1cb elimination can be excluded, as the reaction enthalpy is endothermic by 27·9 and 24·1 kcal mol^{-1} for $ClCH_2^-$ and $BrCH_2^-$, respectively (Table 2).

$$^{A}XCH_2^- \xrightarrow{\alpha\text{-Elimination}} CH_2 + {}^{A}X^- \qquad (3)$$

The next obvious reaction channel is the direct S_N2 substitution of the halomethyl anion on the halomethane [reaction (4a)]. This mechanism leads to the production of the halide anion isotopomers in the proportion of their natural abundance [$I(^{35}Cl^-)/I(^{37}Cl^-) = 3.13$, $I(^{79}Br^-)/I(^{81}Br^-) = 1·03$].[6] Thermodynamically, this direct S_N2 substitution is very favourable as it is exothermic by −72·3 and −74·7 kcal mol^{-1} for X=Cl and Br, respectively (Table 2).

Another conceivable mechanism is the proton transfer-initiated nucleophilic substitution (PT/S_N2) mechanism of the halomethyl anion and ammonia [reaction (4c)]. This PT/S_N2 reaction has first to overcome the phase of endothermic proton transfer, but the overall reaction enthalpy is exothermic by −59·6 and −63·4 kcal mol^{-1} for X=Cl and Br, respectively (Table 2). The PT/S_N2 process produces pure $^{A}X^-$ and thus, overall, leads to an excess of the $^{A}X^-$ isotopomer. The amount with which this process contributes to $I(^{A}X^-)/I(^{B}X^-)$ depends linearly on the pressure ratio $p(NH_3)/p(CH_3X)$. Dissociation of the intermediate structure $XCH_3 \cdots NH_2^-$ is thermodynamically inaccessible [$\Delta H_r(XCH_2^- + NH_3 \rightarrow XCH_3 + NH_2^-) = 7·6$ and 10·9 kcal mol^{-1} for X=Cl and Br, respectively].[14]

Table 2. Overall enthalpies of reaction, ΔH_r (kcal mol^{-1}), for some gas-phase processes of the reaction systems $XCH_2^- + CH_3X + NH_3$(C = Cl, Br)[a]

Equation	Process	ΔH_r(X = Cl)	ΔH_r(X = Br)
3	α-Elimination	27·9	24·1
4a	Direct S_N2	−72·3	−74·7
4b	$S_N2/E2$	−55·1	−56·3
4c	PT/S_N2	−59·6	−63·4
5	S_N2/S_N2	−72·3	−74·7

[a] Calculated from heats of formation given in Ref. 14.

The above-mentioned bimolecular processes [reactions (4a) and (4c)] proceed via dissociation of the product ion–molecule complexes $[^{A}XCH_2CH_3 \cdots X^-]^*$ and $[CH_3NH_2 \cdots {}^{A}X^-]^*$, respectively. While the latter can only dissociate, in the former a secondary $E2$ elimination could take place in which the halide X^- acts as a base and abstracts a β-proton from the haloethane entity with expulsion of the leaving group $^{A}X^-$ [reaction (4b)]. Although this 1,2-elimination step is endothermic (by about 20 kcal mol^{-1} for X=Cl[39]), it can proceed as it is fuelled by the high exothermicity (Table 2) of the foregoing S_N2 step. This can be seen clearly in Figure 1, where the energetics of the reactions between the chloromethyl anion and chloromethane are displayed. The overall $S_N2/E2$ process is exothermic by −55·1 and −56·3 kcal mol^{-1} for X=Cl and Br, respectively (Table 2).

$$^{A}XCH_2^- + CH_3X \rightleftharpoons [^{A}XCH_2^- \cdots CH_3X]^* \xrightarrow{S_N2}$$

$$\rightarrow {}^{A}XCH_2CH_3 + X^- \qquad k_1 \qquad (4a)$$

$$[^{A}XCH_2CH_3 \cdots X^-]^* \xrightarrow{E2}$$

$$[^{A}X^- \cdots C_2H_4 \cdots HX]^* \rightarrow HX + C_2H_4 + {}^{A}X^- \qquad k_2 \qquad (4b)$$

$$^{A}XCH_2^- + NH_3 \rightleftharpoons [^{A}XCH_2^- \cdots NH_3]^* \xrightarrow{PT}$$

$$[^{A}XCH_3 \cdots NH_2^-]^*_{labile} \xrightarrow{S_N2}$$

$$[^{A}X^- \cdots CH_3NH_2]^* \rightarrow CH_3NH_2 + {}^{A}X^- \qquad k_3 \qquad (4c)$$

As the ion–molecule complex $[^{A}XCH_2CH_3 \cdots X^-]^*$ is highly (rovibrationally) excited,[1] entropic factors are expected to play an important role in determining the competition between secondary processes that take place from this complex. Therefore, it is expected that the dissociation of this complex to haloethane and halide [reaction (4a)] dominates over the secondary $E2$ reaction not only owing to the more favourable energetics of the former process, but also because of its looser transition-state structure. Further, the formation of the $[^{A}X \cdots H \cdots X]^-$ clusters is not observed, *i.e.* there is no indication that the entropically less favourable but 20 kcal mol^{-1} more exothermic[14] 1,2-elimination leading to the solvated leaving group takes place.

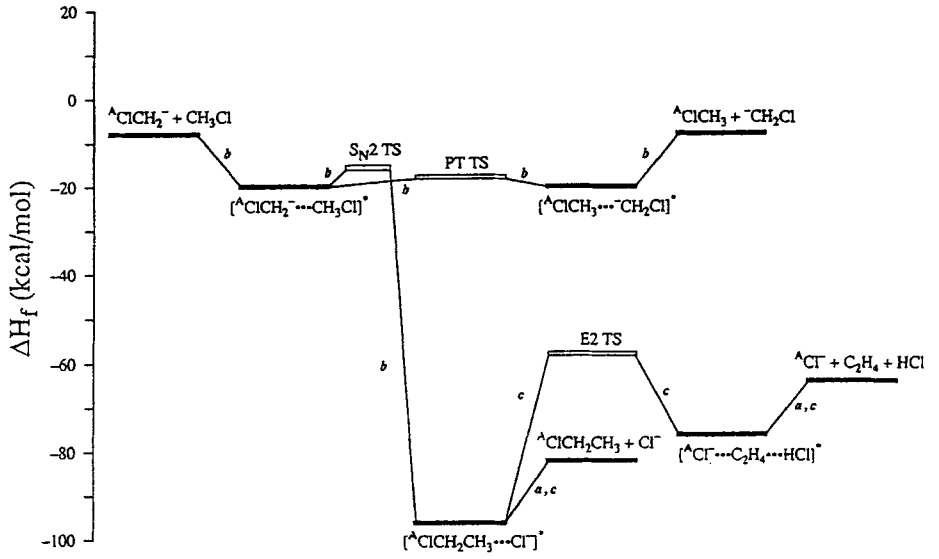

Figure 1. Schematic energy (kcal mol^{-1}) diagram for the thermoneutral proton transfer (PT), the direct S_N2 substitution and the $S_N2/E2$ process of $ClCH_2^-$ and CH_3Cl. The enthalpies of the separated reactants and products, and enthalpy differences with a label *a* were taken from Lias *et al.*[14] The energy differences with a label *b* stem from our own calculations (see Table 4). The energy differences with a label *c* were taken from Minato and Yamabe[39]

Analogous considerations lead to the exclusion of another conceivable secondary reaction occurring in the (rovibrationally) excited[1] $[^AXCH_2CH_3\cdots X^-]^*$ complex, namely the secondary S_N2 substitution of X^- on the haloethane [reaction (5)].

$$[CH_3CH_2{}^AX\cdots X^-]^* \xrightarrow{S_N2} [CH_3CH_2X\cdots {}^AX^-]^* \quad (5)$$

The overall exothermicity of this S_N2/S_N2 reaction is the same as for the direct S_N2 substitution (Table 2). In principle, this process could also make a contribution to the excess of the $^AX^-$ isotopomer which is experimentally indistinguishable from the $S_N2/E2$ contribution [reaction (4b)]. However, although the activation energy for the secondary S_N2 substitution (14·6 kcal mol^{-1}) is 22·7 kcal mol^{-1} lower than that of the $E2$ elimination (37·3 kcal mol^{-1}),[39] the latter reaction might be favoured in the highly (rovibratonally) excited[1] $[^AXCH_2CH_3\cdots X^-]^*$ ion–molecule complex owing to the higher density of states in the 'loose' $E2$ transition state.[40] This assumption is confirmed by studies of our group[3,4] on multi-step gas-phase reactions, in which an intermediate ion–molecule complex occurred that contained both S_N2 and $E2$ reactive sites. In all cases the secondary $E2$ reactions strongly prevail. The facility of $E2$ elimination compared with S_N2 substitution has also been noted in other systems.[15] Finally, also the spatial orientation of the Cl^- in the S_N2 product complex $[^AXCH_2CH_3\cdots X^-]^*$ is in favour of a subsequent $E2$ reaction. The chloride anion is very close to the CH_3 group of the chloroethane and far away from the proper spatial orientation for a 'back-side' attack on the chlorine leaving group which would be necessary for a second S_N2 step.

Summarizing, it is concluded that the three processes in equation (4), i.e. direct S_N2, $S_N2/E2$ and PT/S_N2, can be expected to contribute to the formation of the observed product isotope cluster of halide anions X^- in the reaction system $^AXCH_2^- + CH_3X + NH_3$. On the basis of these possible reactions, equations (6) ($^AX = {}^{35}Cl$) and (7) ($^AX = {}^{79}Br$) can be derived in which the isotope intensity ratio $I(^AX^-)/I(^BX^-)$ is related to the pressure ratio $p(NH_3)/p(CH_3X)$.

$$\frac{I(^{35}Cl^-)}{I(^{37}Cl^-)} = \left(3\cdot13 + \frac{k_2}{k_1}\times 4\cdot13\right) + \left(\frac{k_3}{k_1}\times 4\cdot13\right)\frac{p(NH_3)}{p(CH_3Cl)} \quad (6)$$

$$\frac{I(^{79}Br^-)}{I(^{81}Br^-)} = \left(1\cdot03 + \frac{k_2}{k_1}\times 2\cdot03\right) + \left(\frac{k_3}{k_1}\times 2\cdot03\right)\frac{p(NH_3)}{p(CH_3Br)} \quad (7)$$

As can be seen, the relative magnitude of the overall

rate constants k_1, k_2 and k_3 [reactions (4a), (4b) and (4c), respectively] can be obtained from the slope and the intercept of equations (6) and (7). These can be obtained experimentally by measuring $I(^AX^-)/I(^BX^-)$ as a function of $p(NH_3)/p(CH_3X)$. Finally, one arrives at absolute values for k_1 to k_3 by determining the total rate constant with which the reactant carbanion $^AXCH_2^-$ is transformed to products.

In the case of the chlorine-containing reaction system, the complementary experiment was also carried out with $^{37}ClCH_2^-$ as the reactant carbanion isotopomer ($^AX = {}^{37}Cl$). For this system, equation (8) holds.

$$\frac{I(^{37}Cl^-)}{I(^{35}Cl^-)} = \left(0{\cdot}320 + \frac{k_2}{k_1} \times 1{\cdot}32\right) + \left(\frac{k_3}{k_1} \times 1{\cdot}32\right) \frac{p(NH_3)}{p(CH_3Cl)} \quad (8)$$

RESULTS

Experimental results

In Table 3, the experimentally obtained rate constants k_1, k_2 and k_3 are presented. For the reaction system $ClCH_2^- + CH_3Cl + NH_3$ these constants are $6{\cdot}5 \times 10^{-10}$, $2{\cdot}0 \times 10^{-10}$ and $0{\cdot}78 \times 10^{-10}$ cm^3 molecule^{-1} s^{-1}, respectively. For the reaction system $BrCH_2^- + CH_3Br + NH_3$, k_1, k_2 and k_3 are $7{\cdot}9 \times 10^{-10}$, $1{\cdot}3 \times 10^{-10}$ and $0{\cdot}32 \times 10^{-10}$ cm^3 molecule^{-1} s^{-1}, respectively.

The relative rate constant values (k_2/k_1 and k_3/k_1) for the reaction system $ClCH_2^- + CH_3Cl + NH_3$ stem from three independent experiments with the isotopomer $^{35}ClCH_2^-$ as the reactant carbanion [$^AX = {}^{35}Cl$; equation (6)] and two complementary experiments with $^{37}ClCH_2^-$ [$^AX = {}^{37}Cl$; equation (8)]. Figure 2 shows the $I(^{35}Cl^-)/I(^{37}Cl^-)$ versus $p(NH_3)/p(CH_3Cl)$ graph obtained from the combined 21 data points of the three experiments with $^{35}ClCH_2^-$ together with the $I(^{79}Br^-)/I(^{81}Br^-)$ versus $p(NH_3)/p(CH_3Br)$ graph

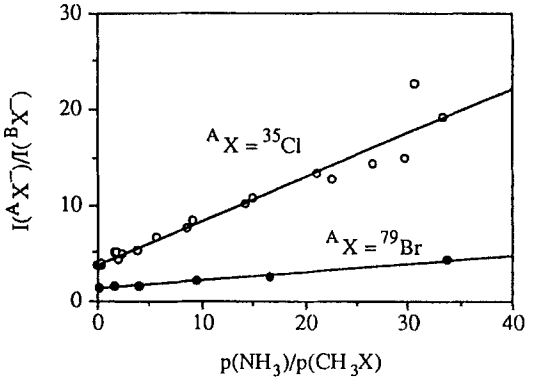

Figure 2. Intensity ratio $I(^{35}Cl^-)/I(^{37}Cl^-)$ as a function of the pressure ratio $p(NH_3)/p(CH_3Cl)$ for the reaction system $^{35}ClCH_2^- + CH_3Cl + NH_3$ (21 data points, three independent series of measurements) and the intensity ratio $I(^{79}Br^-)/I(^{81}Br^-)$ as a function of the pressure ratio $p(NH_3)/p(CH_3Br)$ for the reaction system $^{79}BrCH_2^- + CH_3Br + NH_3$ (six data points, one independent series of measurements)

obtained from the six data points of the experiment with $^{79}BrCH_2^-$ (see below). The error given as a percentage of the ratios k_2/k_1 (45%) and k_3/k_1 (18%) represents the standard deviation over the five independent experiments. The absolute rate constant values were obtained from five separate determinations of the overall rate constant with which $^{35}ClCH_2^-$ is transformed to products and using k_2/k_1 and k_3/k_1. The associated standard deviation is 10%.

The relative rate constant values (k_2/k_1 and k_3/k_1) for the reaction system $BrCH_2^- + CH_3Br + NH_3$ stem from one experiment with the isotopomer $^{79}BrCH_2^-$ as the reactant carbanion [$^AX = {}^{79}Br$; equation (7); see Figure 2). The error given as a percentage of the ratios k_2/k_1 and k_3/k_1 is taken from the five independent experiments for X=Cl. The absolute rate constant values were obtained from three separate determinations of

Table 3. Absolute and relative overall constants k_1, k_2 and k_3 (10^{-10} cm^3 molecule^{-1} s^{-1}) determined for reactions (4a), (4b) and (4c), respectively, of the reaction systems $XCH_2^- + CH_3X + NH_3$ (X = Cl, Br)

			k_i(X=Cl)		k_i(X=Br)	
Equation	Process		Absolute[a]	Relative[b]	Absolute[c]	Relative[d]
4a	Direct S_N2	k_1	6·5 ± 0·6	1·0	7·9 ± 1·7	1·0
4b	S_N2/E_2	k_2	2·0 ± 0·2	0·34 ± 0·14	1·3 ± 0·3	0·16 ± 0·07
4c	PT/S_N2	k_3	0·78 ± 0·08	0·12 ± 0·02	0·32 ± 0·07	0·04 ± 0·01

The indicated experimental error corresponds to the standard deviation of:
[a] 10% over five determinations of the overall rate constant.
[b] 45% [equation (4b)] and 18% [equation (4c)] over five experiments.
[c] 21% over three determinations of the overall rate constant.
[d] 45% [equation (4b)] and 18% [equation (4c)] taken from the five experiments for the chlorine-containing reaction systems (X = Cl). See also the section on the experimental results.

the overall rate constant with which $^{79}BrCH_2^-$ is transformed to products and using k_2/k_1 and k_3/k_1. The associated standard deviation is 21%.

Theoretical results

The theoretical results for the chlorine-containing reaction systems are presented in Tables 4 (energies, charges) and 5 (populations), and in Figures 3 (structures) and 4 (reaction profile for the PT/S_N2 reaction taking place from $[ClCH_2^- \cdots NH_3]^*$). In Table 4 relative energies, ΔE_{rel}, and cluster energies, ΔE_{clust}, are collected. The two reactant anion–molecule complexes $[ClCH_2^- \cdots CH_3Cl]^*$ and $[ClCH_2^- \cdots NH_3]^*$ appear to have comparable cluster energies of $-10{\cdot}84$ and $-10{\cdot}15$ kcal mol^{-1}, respectively. From a bonding energy analysis[30] it appears that the bonding interactions (electrostatic and orbital interaction) are provided for more than 45% by the orbital interaction. This orbital interaction is mainly attributed to the charge transfer from the lone-pair orbital of the carbanion to the σ^*_{C-H} or σ^*_{N-H} MO of the neutral. From Table 5 it appears that in $[ClCH_2^- \cdots NH_3]^*$ the σ^*_{N-H} of NH_3 is populated by 0·19 electrons. Overall both the NH_3 fragment in $[ClCH_2^- \cdots NH_3]^*$ and the CH_3Cl fragment in $[ClCH_2^- \cdots CH_3Cl]^*$, have acquired a charge of about $-0{\cdot}2$ electrons (Table 4). The population of the anti-bonding σ^*_{C-H} and σ^*_{N-H} MOs is also revealed by the elongation of the corresponding bonds by 5·1 pm to $d(C-H)_1 = 115{\cdot}5$ pm and by 7·5 pm to $d(N-H) = 110{\cdot}8$ pm in CH_3Cl and NH_3, respectively (Figure 3), with respect to the isolated fragments. Therefore, it is concluded that the cluster energy for the anion–molecule complexes is provided to a considerable extent by hydrogen bond formation.

In Figure 4 the Xα energy profile for the PT/S_N2 reaction which takes place from the $[ClCH_2^- \cdots NH_3]^*$ reactant ion–molecule complex is depicted. This energy profile is obtained by elongation in steps of 10 pm of the N—H bond which participates in the hydrogen bond and which serves as the reaction coordinate; for every step the Xα energy is calculated after the geometry of the complete system, except for the fixed N—H bond, has been allowed to relax. The graphic representation in Figure 4 starts with the equilibrium value of 110·8 pm for d(N—H) in the reactant anion–molecule complex. When d(N—H) is increased, the (relative) energy ΔE_{rel} rises. Around

Table 4. Calculated relative energies, ΔE_{rel}, and cluster energies (energy change when the weakly bound (···) fragments are brought together), ΔE_{clust}, (kcal mol^{-1}) and fragment charges, Q (fragment), (electrons) for selected chlorine-containing reaction systems[a]

System	ΔE_{rel}[b]	ΔE_{clust}[c]	$Q(A^-)$[d]	$Q(M)$[d]
Chloromethane clusters:				
$[ClCH_2^- \cdots CH_3Cl]^*$	0·00	−10·84	−0·80	−0·20
$[ClCH_2^- \cdots H^+ \cdots {}^-CH_2Cl]^{\neq}$	2·08	–	–	–
Ammonia clusters:				
$[ClCH_2^- \cdots NH_3]^*$	0·00	−10·15	−0·79	−0·21
$[ClCH_3 \cdots NH_2^-]^*_{labile}$	4·31	–	−0·65	−0·35
$[ClCH_3 \cdots NH_2^-]^{\neq}$	7·24	–	−0·74	−0·26
$[CH_3NH_2 \cdots Cl^-]^*$	−56·01[e]	−6·39	−0·84	−0·16

[a] See Figure 3 for structures.
[b] Calculated with Xα exchange-correlation potential.[7]
[c] Calculated with more sophisticated density-functionals[21-25] (see text).
[d] $Q(A^-)$: charge of anionic fragment, $Q(M)$: charge of molecular fragment.
[e] Calculated for the most stable conformation of $[CH_3NH_2 \cdots Cl^-]^*$ with the sophisticated density-functionals[21-25] (see text).

Table 5. Calculated Mulliken MO populations, $P(MO)$, (electrons) for selected chlorine-containing reaction systems on the reaction coordinate of the PT/S_N2 process which takes place from the reactant anion–molecule complex $[ClCH_2^- \cdots NH_3]^*$[a]

System	$P(C_{LP})$	$P(\sigma^*_{N-H})$	$P(N_{LP1})$[b]	$P(N_{LP2})$[c]	$P(\sigma^*_{C-Cl})$	$P(\sigma^*_{C-H})$
$[ClCH_2^- \cdots NH_3]^*$	1·78	0·19				
$[ClCH_3 \cdots NH_2^-]^*_{labile}$			1·76	1·88	0·14	0·14
$[ClCH_3 \cdots NH_2^-]^{\neq}$			1·78	1·96	0·16	0·05

[a] See Figure 3 for structures.
[b] Nitrogen lone pair (NH_2^- HOMO); points to the C—Cl axis at the 'back-side' of the C—Cl bond.
[c] Nitrogen lone pair (NH_2^- HOMO-1); points to the hydrogen of the C—H bond.

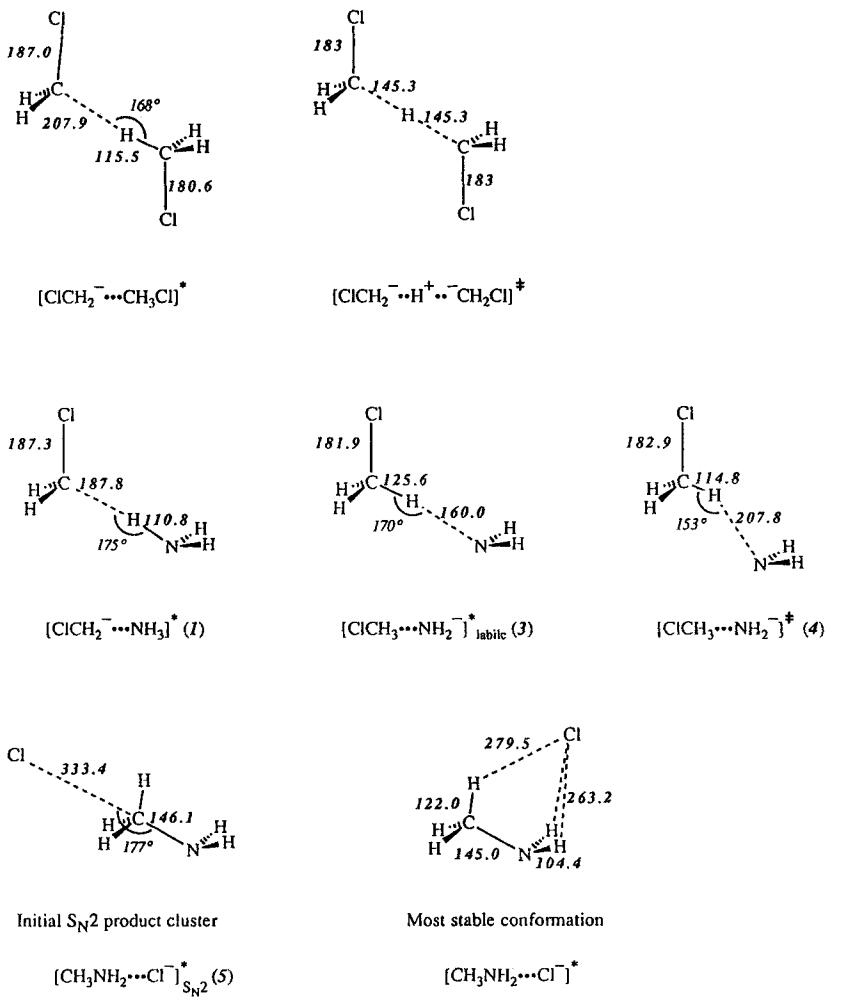

Figure 3. Calculated structure for selected species with C = Cl. Bond lengths (pm) are represented in bold italic and bond angles in italic type

d(N—H) = 160 pm the slope of ΔE_{rel} has a local minimum. At this point the distance d(C—H) is 125·6 pm and the proton can be conceived to be abstracted from ammonia and transferred to the chloromethyl anion. This means that the system now has to be considered as an anion–molecule complex of chloromethane and amide, $[ClCH_3 \cdots NH_2^-]^*$, with an energy of +4·31 kcal mol^{-1} above that of the original reactant complex. However, no energy barrier has been encountered upon formation of this intermediate complex, i.e. $[ClCH_3 \cdots NH_2^-]^*$ is a labile structure without a barrier towards the reformation of the original reactant complex and will therefore be denoted as '$[ClCH_3 \cdots NH_2^-]^*_{labile}$'. However, it is emphasized that there is an entropic bottleneck. This is revealed by the behaviour of the total distance d(C—N) = d(C—H) + d(N—H) which is also represented in Figure 4. In $[ClCH_2^- \cdots NH_3]^*$ and $[ClCH_3 \cdots NH_2^-]^*_{labile}$, d(C—N) is 298·6 and 285·6 pm, respectively. During the proton transfer from nitrogen to carbon, d(C—N) contracts. On the reaction path, between the reactant and the intermediate complex [d(N—H) ≈ 140 pm], one arrives at a minimum for d(C—N) of 279·8 pm. This can be conceived as a tight transition structure that corresponds to a situation with a low density of states, i.e. the just-mentioned entropic bottleneck.

The bond between the amide anion and the chloromethane fragment in $[ClCH_3 \cdots NH_2^-]^*_{labile}$ is, to a considerable extent, due to the hydrogen bond

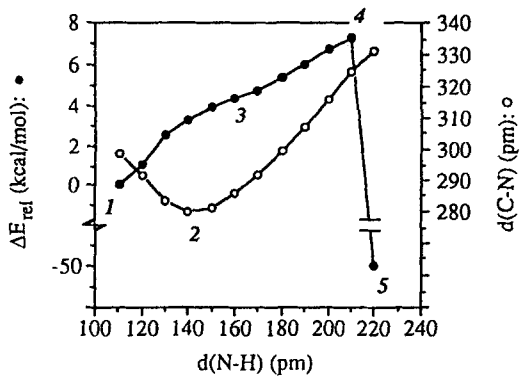

Figure 4. Calculated reaction profile for the PT/S_N2 reaction which takes place from $[ClCH_2^- \cdots NH_3]^*$. In the diagram the relative energy ΔE_{rel} (kcal mol^{-1}) of the system (•) and the distance $d(C-N) = d(C-H) + d(N-H)$ (pm) (○) are displayed as functions of the reaction coordinate $d(N-H)$ (pm). The locations of the following structures are indicated: (1) $[ClCH_2^- \cdots NH_3]^*$; (2) the tight transition structure of the PT phase; (3) $[ClCH_3 \cdots NH_2^-]^*_{labile}$; (4) $[ClCH_3 \cdots NH_2^-]^{\neq}$; and (5) the initial S_N2 product cluster $[CH_3NH_2 \cdots Cl^-]^*_{S_N2}$ (see Figure 3 for structures)

between one lone pair (LP2) of NH_2^- and the σ^*_{C-H} of CH_3Cl, which as a result is populated by 0·14 electrons. Simultaneously, however, the second lone pair (LP1) of NH_2^- already exhibits a considerable charge-transfer interaction with the antibonding σ^*_{C-Cl} of CH_3Cl, resulting in a population of $P(\sigma^*_{C-Cl}) = 0{\cdot}14$ electrons (Table 5). The corresponding bond length, $d(C-Cl)$, has been expanded by 5·6 pm with respect to isolated chloromethane [$d(C-Cl) = 176{\cdot}3$ pm] to 181·9 pm.

On further elongation of $d(N-H)$, the energy still rises at about 210 pm the transition state (TS) of the PT/S_N2 reaction, $[ClCH_3 \cdots NH_2^-]^{\neq}$, is reached, having an activation energy of 7·24 kcal mol^{-1} with respect to the reactant anion–molecule complex (Table 4). Simultaneously, the overall charge transfer from NH_2^- to CH_3Cl decreases from 0·35 electrons in the labile intermediate structure, $[ClCH_3 \cdots NH_2^-]^*_{labile}$, to 0·26 electrons in the TS (Table 4). From an analysis it follows that this mainly results from the breaking of the hydrogen bond between the amide anion and chloromethane. This is also exhibited by the considerable decrease in the population of σ^*_{C-H} from 0·14 electrons in $[CH_3Cl \cdots NH_2^-]^*_{labile}$ to 0·05 electrons in $[CH_3Cl \cdots NH_2^-]^{\neq}$. During the elongation of the bond length $d(N-H)$, the bond angle $\angle(CHN)$ gradually decreases from 175° in $[ClCH_2^- \cdots NH_3]^*$ via 170° in $[ClCH_3 \cdots NH_2^-]^*_{labile}$ to 153° in the TS $[CH_3Cl \cdots NH_2^-]^{\neq}$. This bending displays the beginning of the nucleophilic attack of the NH_2^- HOMO lone pair (LP1) on the antibonding σ^*_{C-Cl} of CH_3Cl. However, whereas in $[ClCH_3 \cdots NH_2^-]^{\neq}$ the hydrogen bond is considerably weakened, the charge transfer to the antibonding σ^*_{C-Cl} of chloromethane, i.e. the nucleophilic attack, is only slightly increased to 0·16 electrons. Also, $d(C-Cl)$ is only slightly increased to 182·9 pm in the TS. It is interesting that already in $[ClCH_3 \cdots NH_2^-]^{\neq}$ the staggered conformation of the aminomethane fragment in the final product anion–molecule complex $[CH_3NH_2 \cdots Cl^-]^*$ can be perceived (Figure 3). In this situation the second lone pair (LP2) points away from the chloromethane fragment and is involved only to a minor extent in charge-transfer interactions to CH_3Cl [$P(LP2) = 1{\cdot}96$ electrons].

When proceeding from $[ClCH_3 \cdots NH_2^-]^{\neq}$, the N—H bond is increased by a further 10 pm to $d(N-H) \approx 220$ pm, the transition state is passed and the nucleophilic substitution of NH_2^- on CH_3Cl proceeds without any further barrier towards the initial product anion–molecule complex, indicated as $[CH_3NH_2 \cdots Cl^-]^*_{S_N2}$ (Figure 3). At this point it is emphasized that the sharp decrease in ΔE_{rel} when the TS is passed (Figure 4) is the result of the choice of $d(N-H)$ as the reaction coordinate throughout the energy profile. If, for example, $d(C-N)$ were to have been employed as the reaction coordinate, a smaller decrease in ΔE_{rel} when going from the TS to the initial product anion–molecule complex would have resulted. In $[CH_3NH_2 \cdots Cl^-]^*_{S_N2}$, aminomethane and the chloride anion are weakly bound by a cluster energy of $-1{\cdot}96$ kcal mol^{-1}. However, in the most stable conformation, $[CH_3NH_2 \cdots Cl^-]^*$ (Figure 3), the cluster energy is $-6{\cdot}39$ kcal mol^{-1} (Table 4). In $[CH_3NH_2 \cdots Cl^-]^*$, the orbital interaction between the anion and the neutral species only provides 36% of the bonding interactions (electrostatic and orbital interaction). Further, in $[CH_3NH_2 \cdots Cl^-]$ only 0·16 electrons have been transferred from the anion to the neutral species, whereas in $[ClCH_2^- \cdots NH_3]^*$ this value is 0·21 electrons (Table 4). Therefore, it is concluded that hydrogen bonding in $[CH_3NH_2 \cdots Cl^-]^*$ is clearly less important than in the reactant complex $[ClCH_2^- \cdots NH_3]^*$. This result parallels the conclusion of Larson and McMahon[41] that electrostatic effects are far more pronounced in anion–molecule complexes with Cl^- than in anion–molecule complexes with F^-. Overall, the transformation of the reactant complex $[ClCH_2^- \cdots NH_3]^*$ to the product complex $[CH_3NH_2 \cdots Cl^-]^*$ is calculated to be exothermic by $-56{\cdot}01$ kcal mol^{-1} (Table 4).

Finally, the reaction path for the thermoneutral proton transfer from chloromethane to the chloromethyl anion in the reactant anion–molecule complex $[ClCH_2^- \cdots CH_3Cl]^*$ is considered. In the reactant complex the bond length $d(C-H)_1$ of the C—H bond in the chloromethane fragment which participates in the hydrogen bond is 115·5 pm, whereas the hydrogen bond length $d(C-H)_2$ between the same H atom and the carbon of the chloromethyl anion is

207·9 pm. The C—H—C hydrogen bond is slightly bent, having an angle of 168°.

When $d(C-H)_1$ is enlarged, the energy of the system increases until the TS for PT, $[ClCH_2^- \cdots H^+ \cdots {}^-CH_2Cl]^{\neq}$, is reached at 2·08 kcal mol^{-1} above the reactant complex. Going from the reactant complex to the TS, the hydrogen bond becomes linear, and the distance $d(C-C) = d(C-H)_1 + d(C-H)_2$ contracts from 323·4 to 290·6 pm. In $[ClCH_2^- \cdots H^+ \cdots CH_2Cl]^{\neq}$ the proton which is to be transferred is located symmetrically between the carbon atoms of both chloromethyl anion fragments [$d(C-H)_1 = d(C-H)_2 = 145·3$ pm]. The considerable contraction (32·8 pm) of $d(C-C)$ indicates that $[ClCH_2^- \cdots H^+ \cdots {}^-CH_2Cl]^{\neq}$ represents not only an energetic barrier but also a tight transition structure with a low density of states, i.e. an entropic bottleneck.

For economic reasons, the reaction path for the S_N2 substitution of the chloromethyl anion on chloromethane in $[ClCH_2^- \cdots CH_3Cl]^*$ has not been fully explored. However, when $ClCH_2^-$ is placed on the C_{3v} axis of CH_3Cl at the 'back-side' of the C—Cl bond, it appears that the nucleophilic substitution proceeds without a barrier, analogously to the situation for the S_N2 reaction of NH_2^- on CH_3Cl. The origin of the barrier for the S_N2 process in $[ClCH_2^- \cdots CH_3Cl]^*$ is therefore ascribed to the breaking of the hydrogen bond in order to bring the nucleophile to the right position for the 'back-side' attack on the C—Cl bond in the substrate. As an estimate for this energy barrier one can take the energy difference of 2·93 kcal mol^{-1} between $[ClCH_3 \cdots NH_2^-]^*_{labile}$ and $[ClCH_3 \cdots NH_2^-]^{\neq}$.

DISCUSSION

The FT-ICR experiments on the two reaction systems $^AXCH_2^- + CH_3X + NH_3$, with X = Cl or Br have revealed that three reaction mechanisms are active (Table 3). (i) Clearly, the dominating process is the direct S_N2 substitution of the halomethyl anion on halomethane in the reactant anion–molecule complex $[XCH_2^- \cdots CH_3X]^*$ [Reaction (4a)], which has an overall rate constant k_1 of $6·5 \times 10^{-10}$ and $7·9 \times 10^{-10}$ cm^3 molecule^{-1} s^{-1} for X = Cl and Br, respectively. (ii) The second process is the $S_N2/E2$ reaction, starting from the same reactant complex [reaction (4b)], and having an overall rate constant k_2 of $2·0 \times 10^{-10}$ and $1·3 \times 10^{-10}$ cm^3 molecule^{-1} s^{-1} for X=Cl and Br, respectively, (iii) The third process, the PT/S_N2 reaction which takes place from the reactant anion–molecule complex $[XCH_2^- \cdots NH_3]^*$ [reaction (4c)], is in both reaction systems considerably slower than the two other reactions, having a rate constant k_3 of $0·78 \times 10^{-10}$ and $0·32 \times 10^{-10}$ cm^3 molecule^{-1} s^{-1} for X=Cl and Br, respectively.

In fact, the direct S_N2 [reaction (4a)] and $S_N2/E2$ process [reaction (4b)] proceeds via a common first reaction step, the nucleophilic substitution. Within the steady-state approximation it can be derived that the rate constant k_{nuc} associated with this elementary reaction is simply given by the sum of the two overall rate constants, i.e. $k_{nuc} = k_1 + k_2$. For X=Cl and Br, k_{nuc} amounts to $8·5 \times 10^{-10}$ and $9·2 \times 10^{-10}$ cm^3 molecule^{-1} s^{-1}, respectively. The corresponding average dipole orientation (ADO) reaction efficiencies[42–44] (k_{nuc}/k_{ADO}) are 0·51 and 0·74, respectively. (Atomic masses and dipole moments [$\mu_D(CH_3Cl) = 1·87$ D, $\mu_D(CH_3Br) = 1·81$ D] used for the ADO calculations were taken from Ref. 6. Polarizabilities [$\alpha(CH_3Cl) = 4·56$ Å^3, $\alpha(CH_3Br) = 5·61$ Å^3] used for the ADO calculations were taken from Ref. 19.) Thus, the S_N2 step proceeds slightly more efficiently for the bromine-containing reaction system, in line with the slightly more favourable thermodynamics (Table 2) and the better leaving group ability of Br compared with Cl.

The ratio k_2/k_1 displays the efficiency with which the secondary $E2$ reaction takes place from the S_N2 product complex, $[XCH_2CH_3 \cdots X^-]^*$, [equation (4b)] competes with the simple dissociation which determines the direct S_N2 process [equation (4a)]. From Table 3, it appears that this efficiency is significantly higher for X = Cl ($k_2/k_1 = 0·34$) than for X = Br ($k_2/k_1 = 0·16$). The higher efficiency of the secondary $E2$ reaction in $[XCH_2CH_3 \cdots X^-]^*$ for the chlorine-containing reaction system can be ascribed to the combined effects of Cl^- being a better elimination base than Br^- and $[ClCH_2CH_3 \cdots Cl^-]^*$ being a more strongly bound cluster ($\Delta H_{clust} = -14·5$ kcal mol^{-1}) than $[BrCH_2CH_3 \cdots Br^-]^*$ ($\Delta H_{clust} = -11·6$ kcal mol^{-1}).[14]

Next, the question is addressed why the (inherently) thermoneutral PT from CH_3X to $^AXCH_2^-$ [equation (1b) for X=Cl] is not observed, as follows from the absence of $^BXCH_2^-$ in the FT-ICR product anion spectra. In principle, the absence of $^BXCH_2^-$ could also be explained by an alternative mechanistic model. (a) PT in $[^AXCH_2^- \cdots CH_3^BX]^*$ does occur and results in the formation of the metastable intermediate product complex $[^AXCH_3 \cdots {}^-CH_2^BX]^*$; (b) subsequently, from this intermediate complex only direct S_N2 and S_N2/E_2 reactions proceed, i.e. dissociation makes no significant contribution. Overall, this model leads to multi-step PT/S_N2 and PT/$S_N2/E2$ mechanisms. However, from the ADO reaction efficiencies (see above) it follows that this hypothesis is incorrect. For example, in the case of X = Cl about half of the collision complexes dissociates without reaction ($k_{nuc}/k_{ADO} = 0·51$). This implies that also half of the product complexes $[^{35}ClCH_3 \cdots {}^-CH_2Cl]^*$, possibly formed from $[^{35}ClCH_2^- \cdots CH_3Cl]^*$ by PT, should dissociate. If thermoneutral PT in $[^{35}ClCH_2^- \cdots CH_3Cl]^*$ were to occur to a substantial extent, then the formation of $^{37}ClCH_2^-$ should be detectable. As this is not the case, it is therefore concluded that indeed this thermoneutral PT cannot compete effectively with the nucleophilic

substitution step, i.e. with the direct S_N2 and the $S_N2/E2$ mechanisms.

From the theoretical calculations on the chlorine-containing reaction system (X = Cl), it follows that the energy barrier for PT in (rovibrationally) excited[1] $[ClCH_2^- \cdots CH_3Cl]^*$ is about 2 kcal mol^{-1}, which is in principle not very high. However, the energy barrier for the S_N2 reaction is also low and is estimated to be only slightly higher (about 3 kcal mol^{-1}; see Figure 1 for a schematic overview of the energetics of all processes that take place from $[ClCH_2^- \cdots CH_3Cl]^*$). This means that there is no sharp energy criterion determining which reaction prevails. Therefore, it is concluded that the decisive factor is the entropic bottleneck associated with the PT.

The theoretical calculations have indicated that the origin of the S_N2 energy barrier is the breaking of the hydrogen bond in $[ClCH_2^- \cdots CH_3Cl]^*$ and $[ClCH_3 \cdots NH_2^-]^*$ in order to bring the anionic fragment to the right position for a 'back-side' nucleophilic attack on CH_3Cl, and that the substitution itself proceeds without an energy barrier. It is interesting that this opens up the possibility of having anion–molecule collisions between $ClCH_2^-$ and CH_3Cl in which the S_N2 reaction occurs instantaneously without an energy barrier, and without the initial formation of a hydrogen-bonded reactant complex that is necessary for PT. These conclusions are completely in line with a theoretical study of Sheldon *et al.*[45] on the S_N2 reaction which takes places between CH_3OH and $CH_3OH_2^+$ with the formation of protonated dimethyl ether and water.[46] From this study,[45] it follows that the main source of the energy barrier for the S_N2 process taking place from the stable reactant cation–molecule complex $[CH_3OH \cdots {}^+H-HOCH_3]^*$ is the breaking of the hydrogen bond between the methanol oxygen and an oxonium hydrogen in order to bring methanol to the right orientation for a 'back-side' nucleophilic attack on $CH_3OH_2^+$. However, the substitution itself shows also a small barrier, contrasting the situation for our anionic systems (see above).

As the last aspect, the proton transfer-initiated nucleophilic substitution (PT/S_N2) reaction which takes place from the reactant anion–molecule complex $[XCH_2^- \cdots NH_3]^*$ is discussed. The rate constant k_3 for the PT/S_N2 reaction has been found to be more than one order of magnitude lower than the rate constant k_{nuc} for the nucleophilic substitution step which takes place in $[XCH_2^- \cdots CH_3X]^*$. The theoretical calculations show that this can be connected with the entropic barrier associated with the PT from ammonia to the halomethylanion and with the relatively high energy barrier that comprises both the endothermicity of the PT in $[XCH_2^- \cdots NH_3]^*$ and the breaking of the hydrogen bond in $[XCH_3 \cdots NH_2^-]^*_{labile}$ that is needed to bring NH_2^- to the right location for a 'back-side' nucleophilic attack on CH_3X. For the PT/S_N2 reaction which starts from $[ClCH_2^- \cdots NH_3]^*$, the energy barrier $\Delta E^{\neq}_{X=Cl}$ is calculated to be $+7{\cdot}24$ kcal mol^{-1}. The energy barrier $\Delta E^{\neq}_{X=Br}$ for the PT/S_N2 reaction in $[BrCH_2^- \cdots NH_3]^*$ has not been calculated. However, as $BrCH_2^-$ has a $3{\cdot}3$ kcal mol^{-1} lower proton affinity (PA)[14] than $ClCH_2^-$, $\Delta E^{\neq}_{X=Br}$ is expected to be a few kcal mol^{-1} higher than $\Delta E^{\neq}_{X=Cl}$ owing to the higher endothermicity of the PT phase of the reaction. This is in accordance with the experimental observation that k_3 for X = Br ($0{\cdot}32 \times 10^{-10}$ cm^3 $molecule^{-1}$ s^{-1}) is less than half that for X = Cl ($0{\cdot}78 \times 10^{-10}$ cm^3 $molecule^{-1}$ s^{-1}).

An interesting result is the fact that the PT/S_N2 reaction is a concerted, one-step process. Although it proceeds via two separate phases, namely PT and S_N2, it passes through only one energetic transition state. This result parallels the finding of Scheiner[13] that the endothermic transfer of a proton from ammonia ($PA = 204{\cdot}0$ kcal mol^{-1})[14] to water ($PA = 166{\cdot}5$ kcal mol^{-1})[14] in the cation–molecule complex $[NH_4^+ \cdots H_2O]^*$ does not lead to a stable complex $[NH_3 \cdots H_3O^+]^*$. From the fact that PT in $[BrCH_2^- \cdots NH_3]^*$ is more endothermic than in $[ClCH_2^- \cdots NH_3]^*$, it is expected that the resulting intermediate structure on the PT/S_N2 reaction path is also labile. This justifies the general notation $[XCH_3 \cdots NH_2^-]^*_{labile}$ for both X = Cl and Br, which has already been employed in the foregoing discussion. Finally, it is pointed out that concerted PT/S_N2 reaction is in perfect agreement with the previous observation[5] that no H–D exchange is observed when $ClCH_2^-$ or $BrCH_2^-$ are allowed to react with ND_3.

REFERENCES

1. N. M. M. Nibbering, *Adv. Phys. Org. Chem.* **24**, 1 (1988).
2. N. M. M. Nibbering, *Acc. Chem. Res.* **23**, 279 (1990).
3. S. Ingemann, N. M. M. Nibbering, S. A. Sullivan and C. H. DePuy, *J. Am. Chem. Soc.* **104**, 6520 (1982).
4. S. Ingemann and N. M. M. Nibbering, *J. Org. Chem.* **48**, 183 (1983).
5. S. Ingemann and N. M. M. Nibbering, *J. Chem. Soc., Perkin Trans. 2* 837 (1985).
6. R. C. Weast (ed.), *CRC Handbook of Chemistry and Physics*, 63rd ed. CRC Press, Boca Raton, FL (1982–83).
7. J. C. Slater, *Quantum Theory of Molecules and Solids*, Vol. 4. McGraw-Hill, New York (1974).
8. R. G. Parr and W. Yang, *Density-Functional Theory of Atoms and Molecules*. Oxford University Press, New York (1989).
9. E. J. Baerends, D. E. Ellis and P. Ros, *Chem. Phys.* **2**, 41 (1973).
10. P. M. Boerrigter, G. te Velde and E. J. Baerends, *Int. J. Quantum Chem.* **33**, 87 (1988).
11. E. J. Baerends and P. Ros, *Chem. Phys.* **8**, 412 (1975).
12. E. J. Baerends and P. Ros, *Int. J. Quantum Chem., Quantum Chem. Symp.* **S12**, 169 (1978).
13. S. Scheiner, *Int J. Quantum Chem.* **23**, 753 (1983).

14. S. G. Lias, J. E. Bartmess, J. F. Liebmann, J. L. Holmes, R. D. Levin and W. G. Mallard, *J. Phys. Chem. Ref. Data* **17**, Suppl. 1 (1988).
15. L. J. de Koning and N. M. M. Nibbering, *J. Am. Chem. Soc.* **109**, 1715 (1987), and references cited therein.
16. L. J. de Koning, C. W. F. Fort, F. A. Pinkse and N. M. M. Nibbering, *Int. J. Mass Spectrom. Ion Processes* **95**, 71 (1989).
17. W. T. Huntress, Jr, J. B. Laudenslager and R. F. Pinizzotto, Jr, *Int. J. Mass Spectrom. Ion Phys.* **13**, 331 (1974).
18. J. E. Bartmess and R. M. Georgiadis, *Vacuum* **33**, 149 (1983).
19. K. J. Miller, *J. Am. Chem. Soc.* **112**, 8533 (1990).
20. L. Versluis and T. Ziegler, *J. Chem. Phys.* **88**, 322 (1988).
21. A. D. Becke, *Int. J. Quantum. Chem.* **23**, 1915 (1983).
22. A. D. Becke, *J. Chem. Phys.* **85**, 7184 (1986).
23. T. Ziegler, V. Tschinke and A. Becke, *Polyhedron* **6**, 685 (1987).
24. H. Stoll, E. Golka and H. Preus, *Theor. Chim. Acta* **55**, 29 (1980).
25. S. H. Vosko, L. Wilk and M. Nusair, *Can J. Phys.* **58**, 1200 (1980).
26. F. M. Bickelhaupt, R. H. Fokkens, L. J. de Koning, N. M. M. Nibbering, E. J. Baerends, S. J. Goede and F. Bickelhaupt, *Int. J. Mass Spectrom. Ion Processes* **103**, 157 (1991).
27. T. Ziegler, V. Tschinke and C. Ursenbach, *J. Am. Chem. Soc.* **109**, 4825 (1987).
28. T. Ziegler, V. Tschinke, L. Versluis and E. J. Baerends, *Polyhedron* **7**, 1625 (1988).
29. L. Fan and T. Ziegler, *J. Chem. Phys.* **92**, 3645 (1990).
30. F. M. Bickelhaupt, N. M. M. Nibbering, E. M. van Wezenbeek and E. J. Baerends, submitted.
31. T. Ziegler and A. Rauk, *Theor. Chim. Acta* **46**, 1 (1977).
32. A. Støgård, A. Strich, J. Almlöf and B. Roos, *Chem. Phys.* **8**, 405 (1975).
33. B. O. Roos, W. P. Kraemer and G. H. F. Diercksen, *Theoret. Chim. Acta* **42**, 77 (1976).
34. Z. Latajka and S. Scheiner, *Int. J. Quantum Chem.* **29**, 285 (1986).
35. G. Caldwell and P. Kebarle, *Can. J. Chem.* **63**, 1399 (1985).
36. J. W. Larson and T. B. McMahon, *J. Am. Chem. Soc.* **105**, 2944 (1983).
37. J. D. Payzant, R. Yamadagni and P. Kebarle, *Can. J. Chem.* **49**, 3308 (1971).
38. M. DePaz, A. G. Giodini and L. Friedman, *Int. J. Mass Spectrom. Ion Phys.* **3**, 465 (1970).
39. T. Minato and S. Yamabe, *J. Am. Chem. Soc.* **110**, 4586 (1988).
40. T. Minato and S. Yamabe, *J. Am. Chem. Soc.* **107**, 4621 (1985).
41. J. W. Larson and T. B. McMahon, *J. Am. Chem. Soc.* **106**, 517 (1984).
42. T. Su and M. T. Bowers, *J. Chem. Phys.* **58**, 3027 (1973).
43. T. Su and M. T. Bowers, *Int. J. Mass Spectrom. Ion Phys.* **12**, 347 (1973).
44. T. Su and M. T. Bowers, *Int. J. Mass Spectrom. Ion Phys.* **17**, 211 (1975).
45. J. C. Sheldon, G. J. Currie and J. H. Bowie, *J. Chem. Soc., Perkin Trans. 2*, 941 (1986).
46. J. C. Kleingeld and N. M. M. Nibbering, *Org. Mass Spectrom.* **17**, 136 (1982).